



**HAL**  
open science

## Impact of relative humidity and temperature oscillations mimicking authentic storage during shipping on whey proteins powders properties

Jennifer Burgain, G. Francius, L. Cvetkovska, Cédric Paris, M. Alexander, C. Ray, S. El-Kirat-Chatel, Claire Gauzelin-Gaiani

### ► To cite this version:

Jennifer Burgain, G. Francius, L. Cvetkovska, Cédric Paris, M. Alexander, et al.. Impact of relative humidity and temperature oscillations mimicking authentic storage during shipping on whey proteins powders properties. *Food Structure*, 2023, 37, pp.100326. 10.1016/j.foostr.2023.100326 . hal-04117153

**HAL Id: hal-04117153**

**<https://hal.univ-lorraine.fr/hal-04117153v1>**

Submitted on 16 Nov 2023

**HAL** is a multi-disciplinary open access archive for the deposit and dissemination of scientific research documents, whether they are published or not. The documents may come from teaching and research institutions in France or abroad, or from public or private research centers.

L'archive ouverte pluridisciplinaire **HAL**, est destinée au dépôt et à la diffusion de documents scientifiques de niveau recherche, publiés ou non, émanant des établissements d'enseignement et de recherche français ou étrangers, des laboratoires publics ou privés.

Copyright

# Impact of relative humidity and temperature oscillations mimicking authentic storage during shipping on whey proteins powders properties

J. BURGAIN<sup>1§</sup>, G. FRANCIUS<sup>2§</sup>, L. CVETKOVSKA<sup>1</sup>, C. PARIS<sup>1</sup>, M. ALEXANDER<sup>3</sup>, C. RAY<sup>3</sup>, S. EL-KIRAT-CHATEL<sup>2</sup> & C. GAIANI<sup>1\*</sup>

<sup>1</sup> Université de Lorraine, LIBio, F-54000, Nancy, France

<sup>2</sup> Université de Lorraine, CNRS, LCPME, F-54000 Nancy, France

<sup>3</sup> Arla Foods Ingredients Group P/S, Sønderupvej 26, 6920 Videbæk, Denmark

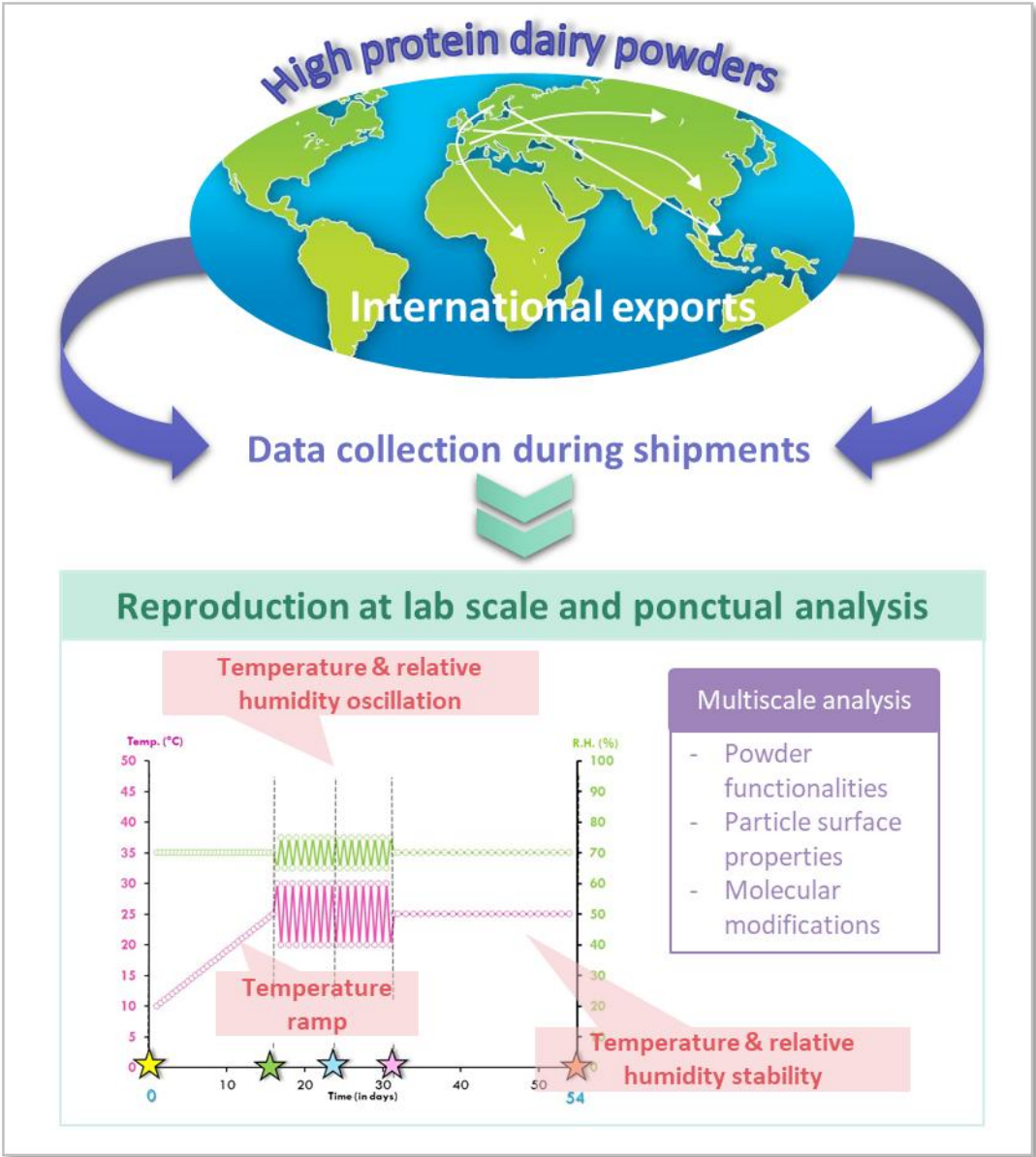
<sup>§</sup>Co-first authors

\*Corresponding author: [claire.gaiani@univ-lorraine.fr](mailto:claire.gaiani@univ-lorraine.fr)

## **Abstract**

The impact of authentic storage conditions during shipping was tested on whey protein concentrate powders as environmental conditions heavily influence shelf-life performance. Most experimental studies are conducted at constant conditions of temperature and/or humidity whereas in real shipment conditions powders are often transported all over the world in ships which can experience vastly different temperatures and humidity with large amplitudes from day-time to night-time. Here, industrial whey protein concentrates and  $\beta$ -lactoglobulin powders were stored under cycled temperatures and relative humidity fashioned from authentic data collected on ships carrying dairy powders. Protein lactosylation and denaturation, browning index, particle surface and powder functional properties were measured in order to estimate functional and physicochemical modifications occurring close to authentic storage under shipping. It was observed that oscillation amplitudes tested had no impact on powders unlike the storage duration. The presence of residual lactose (1.5%) in the whey protein powder induced lactosylation during storage leading to particle surface hydrophobicity and surface elasticity increases whereas for  $\beta$ -lactoglobulin powders (depleted in lactose), transformation of initial lactosylated proteins into advanced Maillard products was observed with no particle surface impact. The rehydration was not impacted regardless of the storage conditions and powder chemical composition.

**Key words:** whey proteins,  $\beta$ -lactoglobulin, lactosylation, denaturation, Maillard reaction, authentic storage conditions, oscillation.



## 1. Introduction

Liquid food products are highly perishable and spray-drying is the favoured process to stabilize dairy ingredients over long periods of time and simultaneously to reduce their volume for cheaper transport. This drying process is used in many fields such as pharmaceutical, nutraceutical, food and particularly for dairy products. Therefore, whatever the context, the aim is to improve stability and extend product shelf-life, and reduce its transport and storage costs (Fang & Bhandari, 2012). The challenge is to maintain the physicochemical, nutritional and functional properties of the dry material through the drying process (Schuck et al., 2016; O'Sullivan et al., 2019) and during storage (Baldwin et al., 2020; Nishanthi et al., 2018).

The impact of spray-drying on food material properties has been investigated in depth in recent years. Conversely, fewer studies were focused on powder authentic storage life whereas the development of the international trade in the recent decades deeply increased. Powder storage stability depends heavily on its intrinsic characteristics as well as the environmental conditions (temperature, relative humidity) to which they are subjected during storage. Even if some studies evidenced that storage conditions can affect the structural and functional properties of dairy powders and more particularly high protein dairy powders (Anema et al., 2006; Burgain et al., 2016b; Gazi & Huppertz, 2015; Nishanthi et al., 2018), few of them mimic authentic storage conditions. In this regard, a major technological challenge is to better understand physicochemical and functional changes during global powder shipping with sometimes significant humidity and temperature oscillations from day-time to night-time (Borocz et al., 2015; Csavajda & Böröcz, 2019).

During shipment and/or storage, a range of physicochemical reactions can lead to protein modification in dairy powders, in particular when they are subjected to elevated temperatures and humidity. For high protein content powders and particularly for whey protein concentrates (WPC), one of the most important storage-induced modification is the Maillard reaction (MR) (Guyomarc'h et al., 2000). In WPC powders, MR is influenced by many factors: temperature, duration, initial pH, water activity ( $a_w$ ), physical state of the matrix and lactose concentration (Baisier & Labuza, 2002). The presence of initial lactosylated proteins into the concentrate (Paul et al., 2022) has also been evidence to induce MR. Denaturation of whey proteins is another type of modification that takes place during storage. These physicochemical changes affect an important number of powder characteristics including

particle size, surface charge, colour, thermal behaviour and morphological character (Norwood et al., 2016).

When elucidating how environment can impact powder properties, powder surface appears to be fundamental for assessing changes in powder functionality as this is the first layer in contact with the environment. Various methodologies have been developed to characterize dairy powder surfaces in order to better understand their functional characteristics (Burgain et al., 2017), particularly Scanning Electron Microscopy (SEM), X-ray Photoelectron Spectroscopy (XPS) (Fournaise et al., 2021; Nishanthi et al., 2018) and more recently Atomic Force Microscopy (AFM) (Burgain et al., 2017; Gaiani et al., 2021). AFM is seldom used in the food powder field in comparison with its use in materials or biological domains. Nevertheless, this technique seems to be highly promising for dairy powders surface characterization at the nanoscale (Burgain et al., 2017; Cardenas-Perez et al., 2019; Yang et al., 2007). AFM has proven to be a relevant tool in surface properties investigation particularly to examine the influence of different environmental conditions such as humidity and/or temperature (Burgain et al., 2017). It also allows simultaneous quantification of nanoscale changes in morphology and surface properties (*e.g.* elasticity and hydrophobicity), which can in some cases be related to storage conditions (Gaiani et al., 2021).

Finally, environment can also strongly impact powder functional properties. Due to its wide range of applications and the demand for high quality milk proteins, powders and more particularly WPC should exhibit good functionalities, *e.g.* rehydration (including wettability, dispersibility and solubility), flowability, viscosity, gelation, thickening, foaming/whipping, and also heat stability (Sharma et al., 2012).

The aim of this paper is to gain an understanding of the impact of the relative humidity and temperature oscillations on the functional and physicochemical properties of whey proteins powders. Most studies are performed at constant storage conditions whereas powders can conceivably experience day-time to night-time environment oscillations during authentic storage. In this study, powder color, protein lactosylation and denaturation and powder surface modifications were monitored under storage conditions mimicking authentic storage. For this purpose, whey protein and  $\beta$ -lactoglobulin powders were stored under cycling temperatures and relative humidity fashioned from authentic data.

## 2. Material and methods

## 2.1. Powders production

Powders were produced and provided by Arla Foods Ingredients (AFI, Videbæk, Denmark) as already detailed by **Gaiani et al., (2021)** and **Paul et al., (2022)**. Three industrial powders were studied. Powders A and B were both whey protein concentrates (entitled WPC A and WPC B in this article) coming from two independent productions but with similar feed content and dried under the same conditions. The third powder was a reference powder mainly composed of  $\beta$ -lactoglobulin (entitled  $\beta$ -LG) and with no detectable residual lactose, individual caseins and/or lipids.

## 2.2 Powder storage to mimic authentic storage conditions

Powder storage was performed in two phytotrons (each dedicated to one oscillation range condition). They allow powder storage in a confined space (20 m<sup>2</sup>) in which the climatic parameters are regulated (temperature and relative humidity). However, lighting (intensity, spectrum, period) and composition of the atmosphere (CO<sub>2</sub>, ozone, etc.) could also be controlled. As a consequence, the two phytotrons were equipped with temperature control and humidifiers generating water vapor.

Real data coming from ship trackers were supplied by AFI and are presented in **Supplementary material S1**. From these authentic data three distinct phases appear, corresponding to first, a temperature (T°C) ramp with constant Relative Humidity (RH), then to T°C and RH oscillations, and finally to constant T°C and RH. Therefore, the phytotrons were programmed to mimic storage with these three phases (**Figure 1**). In the first phase (0 to 16 days), a linear increasing step of temperature is performed from 10 to 25 °C and the relative humidity is maintained at 70 % for both conditions. Then, a second phase was set with temperature and relative humidity oscillations corresponding to day/night periods from day 16 to day 31. Here, large RH (65 – 75 %) and T°C (20 – 30 °C) oscillations are programmed for Large oscillation set and small RH (67.5 – 72.5 %) and T°C (22.5 – 27.5 °C) oscillations are programmed for Small oscillation set. The mean RH and T°C are similar for both conditions and are 70 % and 25 °C respectively. Finally, in the last phase, storage is performed under constant temperature and constant RH from day 31 to 56. During this final phase, the RH is maintained at 70 % and the temperature at 25 °C for both conditions. All these parameters are programmed, continuously monitored and recorded (**Supplementary material S2**). Under these conditions, it is expected to be slightly under the powder T<sub>g</sub> (i.e. T<sub>g</sub> around 35 ± 2 °C at 70 RH).

## Supplementary material S3

### 2.3. Powder color measurement

Powder color was measured with a CR-400 chromameter (Konica Minolta). Around 10 g of powder was poured in a Petri dish. Color was measured according to the three-color coordinates ( $L^*$ ,  $a^*$ ,  $b^*$ ). The  $L^*$  value represents powder luminosity, varying from black (0) to white (100), the  $a^*$  value represents the color varying from red (+) to green (-) and the  $b^*$  value represents the color varying from yellow (+) to blue (-). Browning index (BI) is defined following **eq 1** and is a classical indicator of browning in food powders.

$$BI = 100 * \frac{(x - 0.31)}{0.17} \quad \text{eq 1}$$

$$\text{With } x = \frac{(a^* + 1.75 L^*)}{(5.645 L^* + a^* - 3.012 b^*)}$$

### 2.4. Powder chemical composition

#### 2.4.1 Water content

The water content was determined by the loss of water mass of 1 g powder after drying at 103 °C until a constant dry powder mass was obtained (**AFNOR, 2004**).

#### 2.4.2 Proteins

The nitrogen contents of the powders were determined as previously described by **Schuck et al., (2012)**. The total nitrogen (TN) content, non-casein nitrogen (NCN) content corresponding to the soluble fraction at pH 4.6, and non-protein nitrogen (NPN) content corresponding to the soluble fraction after their precipitation were determined by the Kjeldahl method. Nitrogen contents were converted into protein contents using 6.38 as multiplying factor.

#### 2.4.3 Lipids

Total fat extraction was performed with a method adapted from **Folch et al., (1957)**. Powder (5 g) was dissolved into a mixture of chloroform/methanol (2:1 (v/v)). The mixture was stirred (700 rotation per minutes - rpm) during 15 min. The solvent was then separated by filtration on a sintered glass filter (10 – 16  $\mu\text{m}$  porosity) and recovered in a round-bottom boiling flask. The solvent containing the total fat was removed with a rotary vacuum evaporator (Heidolph



laboratora 4000) at 40 °C and 40 rpm. The boiling flask without solvent was dried in an oven to 103 °C for 10 min to ensure complete evaporation of the solvent and finally weighted.

#### 2.4.4 Ashes

Minerals content was determined by mineralising 2 g of sample at 550 °C during 12 h (Mortensen & Wallin, 1989).

#### 2.4.5. Identification and quantification of native proteins (by RP-HPLC)

Measurement of proteins (*i.e.* residual caseins,  $\beta$ -LG (A),  $\beta$ -LG (B) and  $\alpha$ -LA) was performed by reverse-phase high-performance liquid chromatography (RP-HPLC) as already described by Paul et al., (2022). The HPLC system (Shimadzu Corporation, Kyoto, Japan) was composed of a DGU-20A3 prominence 3 ways-degasser, SCL-10A VP system controller, a LC20-AD pump, a SIL-10AD VP auto-injector and a SPD-M10A VP UV/VIS diode array detector, a regulator and column oven (Croco-cil 100-040-220P, Cluzeau Info Labo). The data were processed on Shimadzu LC solution software. The protein separation was performed using an Agilent (Santa Clara, USA) ZORBAX 300 Extend column (250 mm length x 4.6 mm diameter, C18-bonded silica, 5  $\mu$ m bead size, 30 nm pore size).

The sample was rehydrated at 3 % (w/v) during one hour at 4 °C in ultra-pure water. Protein precipitation was performed by the addition of 1M acetic acid to reach pH 4.6 (solubility criteria). Finally, a centrifugation at 14500 rpm for 25 min was done.

The first mobile phase was polar (A-phase) and composed of ultra-pure water, acetonitrile and trifluoroacetic acid at 89.9 %, 10 % and 0.1 % v/v, respectively. The second mobile phase was non-polar (B-phase) and composed of ultra-pure water, acetonitrile and trifluoroacetic acid at 10 %, 89.9 %, 0.1 % v/v, respectively.

The mobile phase flow rate was maintained at 1 mL.min<sup>-1</sup> and the temperature was set at 25 °C. The pressure was 114 bars and 10  $\mu$ L of sample was injected per analysis. During analysis, the mobile phase was initially composed of 80 % A-phase and 20 % B-phase. During the next first 35 minutes, B-phase was linearly increased from 20 % to 65 %. Then, it was raised up to 100 % from 35 minutes to 45 minutes for finally being decreased to 20 % until 65 minutes.

The quantification was performed using standards curves (as shown in Paul et al., 2022) for  $\beta$ -LG (A and B variant) and  $\alpha$ -lactalbumin ( $\alpha$ -LA).

#### 2.4.6. Protein lactosylation (using UHPLC-MS)

The procedure is the same as already presented by **Paul et al., (2022)**. The samples were rehydrated a day before at 5 % (m/v) at 4 °C in ultra-pure water and acidified with acetic acid (1 M) (255 µl of acid with 1.7 mL of sample). The solutions were vortexed and kept one hour at 4 °C. A centrifugation at 14500 rpm during 25 min was then performed. Finally, the sample was filtrated (0.2 µm) and diluted (1/10) with ultra-pure water.

Qualitative and semi-quantitative analysis of the different lactosylated forms of protein was realized on a UHPLC-MS system (ThermoFisher Scientific, San Jose, CA, USA) consisting in a quaternary U3000 solvent delivery pump connected to a photodiode array detector (PDA) and a LTQ<sup>XL</sup> mass spectrometer equipped with an atmospheric pressure ionization interface operating in electrospray positive mode (ESI<sup>+</sup>). Ten microliters of sample were separated on a C18 Alltima reverse phase column (150 x 2.1mm, 5µm – Grace/Alltech, Darmstadt, Germany) equipped with a C18 Alltima pre-column (7.5 x 2.1mm, 5µm) at 25 °C. The flow rate was set at 0.2 mL.min<sup>-1</sup> and mobile phases consisted in water modified with trifluoroacetic acid (0.1 %) for A and acetonitrile modified with trifluoroacetic acid (0.1 %) for B. Proteins were eluted using a linear gradient from 10 % to 98 % of B for 15 min. Mass spectrometric conditions were as follows: spray voltage was set at + 5 kV; source gases were set (in arbitrary units.min<sup>-1</sup>) for sheath gas, auxiliary gas and sweep gas at 20, 5 and 5, respectively; capillary temperature was set at 350 °C; capillary voltage at + 26 V; tube lens, split lens and front lens voltages at + 130 V, - 42 V and - 5.75 V, respectively.

Ion optics parameters were optimized by automatic tuning using a standard solution of BSA at 0.1 g.L<sup>-1</sup> infused in mobile phase (A/B: 50/50) at a flow rate of 5 µL.min<sup>-1</sup>. Semi-quantitative screening of total soluble proteins was realized using UV230 absorbance. Structural elucidation of the different lactosylated forms of protein was realized thanks to full scan MS spectra performed on LTQ<sup>XL</sup> analyzer from 1500 to 4000 m/z, and subsequent assignment of charge states of proteins.

In addition, semi-quantitative analysis of lactosylated forms was achieved through specific mass spectrometry screening. Raw data were processed using the XCALIBUR software program (version 2.1, <http://www.thermoscientific.com>).

#### 2.5. Rehydration properties

Rehydration ability of the powders was evaluated through wettability, dispersibility and solubility indices. The IDF standards were slightly adapted for wettability, dispersibility (IDF, 1979) and solubility (IDF, 2005).

### 2.5.1 Wettability

Wettability was determined by the time in seconds taken by 13.0 g of powder to become wet when deposited at the surface of 125.0 g distilled water (at 20 °C) in a 250 mL beaker (IDF, 1979).

### 2.5.2 Dispersibility

Dispersibility index was measured by a method adapted from IDF (1979). Powder (13.0 g) was deposited on the surface of 125.0 g distilled water (at 20 °C) placed in a 400 mL beaker. The mixture was first manually stirred for 20 s and then allowed to rest for 30 s. Finally, the mixture was passed through a 120 µm sieve. The total dry matter in the liquid was determined after drying at 103 °C for 5 h following eq 2.

$$\text{Dispersibility (\%)} = \frac{W \times T}{100 - (E + T)} \times \frac{100}{S} \quad \text{eq 2}$$

With:

- W: distilled water mass (g);
- T: dry matter content (% w/w) of the liquid;
- E: dry matter content (% w/w) of the sample;
- S: sample mass (g).

### 2.5.3 Solubility

Solubility was determined by the addition of 2.5 g powder in 17.5 mL distilled water (at 20 °C) in a 50 mL centrifugation tube (IDF, 2005). This step was followed by 30 s stirring and centrifugation at 2 294 x g during 10 min. Then, the supernatant was removed and 20 mL distilled water was added to the pellet, followed by a second stirring (30 s) and centrifugation (2 294 x g during 10 min). The pellet was dried at 103 °C overnight to determine the mass of insoluble residues, which allows determining the solubility index following eq 3.

$$\text{Solubility (\%)} = 100 - \frac{M \times 100}{S} \quad \text{eq3}$$

With:

- M: sediment mass after desiccation (g);
- S: sample mass (g).

## 2.6. Particle surface properties probed by AFM

### 2.6.1. Sample preparation

Prior to AFM experiments, WPC particles were sampled according to the following procedure. WPC particles were immobilized onto a glass disk (35 mm diameter) previously coated with a thin layer of epoxy glue (Araldite® Crystal) spread using a scraper to obtain a flat and thin layer. 5 mg of WPC are spread onto this adhesive substrate and placed into a desiccator under nitrogen flow for 2 hours. Samples were ready after 2 hours when the glue was totally cured.

### 2.6.2. Nanomechanical properties

Mechanical properties of individual particles were probed at the nanoscale by AFM nanoindentation technique. The force-distance curves recorded by AFM were analyzed according to the theoretical Sneddon model to extract the mechanical properties (*e.g.* elasticity) (Burgain et al., 2017; Gaiani et al., 2021; Prime et al., 2011). Using a MFP3D-BIO instrument (Asylum Research Technology, Oxford Instrument, Manheim, Germany), defined areas were probed to generate elasticity maps. Measurements were performed in air and at room temperature with stiff cantilevers (RTESPA with ~200 N/m spring constant). The cantilever was calibrated onto sapphire wafers. At least 12 particles were analyzed per sample by recording elasticity maps of 256 or 1024 force curves on areas of 10 μm × 10 μm. All maps were processed under Matlab™ using an automated algorithm previously described by Polyakov et al., (2011).

### 2.6.3. Surface hydrophobicity by chemical force microscopy

The effect of storage on particles surface hydrophobicity was probed by AFM-based chemical force microscopy (CFM). Hydrophobicity measurements were performed in ethanol to avoid powder rehydration and using gold-coated AFM tips (NPG-10, Bruker AXS, Palaiseau, France,

spring constant  $\sim 0.12$  N/m) previously functionalized with alkanethiols by passive immersion in a solution of 1 mM dodecanethiol during 14h in the dark. Before each experiment, functionalized AFM-tips efficiency was systematically tested and calibrated onto hydrophobic coated gold substrates prepared at the same time (Alsteens et al., 2007). Adhesion maps were obtained from the automated analysis of force distance curves recorded for each sample. Each map corresponds to the analysis of 1024 force distance curves on areas of  $10 \mu\text{m} \times 10 \mu\text{m}$ . Data were analyzed using Nanoscope Analysis 1.8 software and Matlab<sup>TM</sup>.

## 2.7. Statistical analysis

The two WPC batches presenting the same formulation were spray-dried independently leading to the studied powders: powder WPC A and powder WPC B. The  $\beta$ -LG powder was spray-dried in the same conditions. For each powder, 2 independent experiments of 3 measurements were performed. The repeatability can thus be estimated by the 3 measurements performed on different location of the same sample and reproducibility is evaluated through the comparison of results between independent powders. Data were reported as mean values plus standard error of the mean of at least three replicates. The significance level using a paired two-tailed Student's t-test was set to P values N.S. (non-significant)  $> 0.05$ , \*P  $\leq 0.05$ , \*\*P  $\leq 0.01$ , and \*\*\*P  $\leq 0.001$ .

## 3. Results

### 3.1. Impact of storage on powder chemical properties

#### 3.1.1 Chemical composition

The chemical composition of fresh powders was evaluated (Table 1). It can first be observed that, as expected, the composition of powders WPC (A) and (B) are very similar. Proteins represent the major constituents with 74.8 and 76.8 % for WPC (A) and (B), respectively. In the proteins fraction,  $\beta$ -LG (variant A),  $\beta$ -LG (variant B) and  $\alpha$ -LA are measured and present similar percentages of total protein,  $\sim 25$  %,  $\sim 47$  % and  $\sim 28$  %, respectively. Residual lipids (4 – 5 %) and lactose (1.5 %) are also found. The  $\beta$ -LG powder has a high protein content (83.9 %) and no lipids or lactose are detected. In the  $\beta$ -LG powder,  $\beta$ -lactoglobulin variants represent the major constituent of proteins and no residual individual caseins or  $\alpha$ -LA remain in this control powder.

The WPC composition was found to be similar to that determined by **Paul et al., (2022)** on different batches coming from the same company with the same process whereas the  $\beta$ -LG powder is coming for the same batch and presents, therefore, exactly the same composition.

### 3.1.2 Maillard reaction indicator

The MR is known to be one of the major deteriorative reactions during storage and particularly for food powders. In that case, the powder appearance changed with the development of a brown color due to the production of melanoidins. An easy way to evaluate the Maillard reaction development is the measurement of colorimetric parameters with the calculation of the BI (**Figure 2-A**). Images of powders spread in Petri dishes during storage were taken for each oscillation condition (**Figure 2-B**). From these images and BI values, it is clearly visible that WPC powders does not change significantly during storage. Indeed, the BI increase (between 0 and 56 days of storage) is only about 1.0 % whatever the storage oscillation. These results mean that the color does not change during powder storage with large or small temperature and humidity oscillations. It is also confirmed by images of powders poured in Petri dishes with no visual differences (**Figure 2-B**). On the contrary, for  $\beta$ -LG powder, a powder devoid of lactose and lipid traces, even if the initial BI was low, the BI increased significantly during storage (3.5 %). Nevertheless, even if the BI increase is significant between 0 and 56 days of storage; it is exactly the same evolution for conditions of small and large oscillations. These results mean that the oscillations during storage had no impact on color change and that only storage duration had an impact.

The lactose content was already shown to have a significant effect on whey protein powders ageing (**Norwood et al., 2017**) and the development of the brown color. It was not the case in this study as the BI increase is observed only for  $\beta$ -LG powder which is lactose depleted and not observed for WPC powders containing around 1.5 % lactose. These results may be explained by first the temperature of storage and second the presence of lactosylated proteins in the initial  $\beta$ -LG powder. For a given powder, the browning rate increases exponentially with increasing T-Tg (T being the storage temperature and Tg the glass transition temperature of the powder) (**Paul et al., 2022**). The Tg of the powders at 70 RH is around  $35 \pm 2$  °C meaning that all storage conditions ( $25 \pm 5$  °C for large oscillations and  $25 \pm 2.5$  °C for small oscillations) are below this critical value and explaining the absence of browning for WPC powders. This Tg value was in agreement with those of **O'Donoghue et al.,**

(2020) studied on WPC 20-65 between 0.11 and 0.44 RH. Nevertheless, in this study the BI values increased for  $\beta$ -LG powder. It may be hypothesised that due to the different processes applied to the  $\beta$ -LG concentrate, the presence of initial lactosylated proteins are engaged in Maillard reaction during storage leading to the production of brown pigments. Due to the “white” color of the powder with a low initial BI index, even low quantities of lactosylated proteins engaged in Maillard reaction may be detected. Paul et al., (2022) demonstrated that browning was independent to the initial lactose content and they observed a BI increase for powders containing undetectable levels of lactose. BI increase was measured by these authors for WPC powders but the storage temperatures were significantly higher and superior to the powder Tg which is not the case in this work.

### 3.1.3 Protein denaturation and lactosylation

To validate or reject the precedent hypothesis, protein denaturation and lactosylation for WPC and  $\beta$ -LG powders were determined for the two storage conditions.

Soluble proteins (native) were quantified by RP-HPLC (Figure 3). The mean values were calculated from data obtained for WPC A and B. The values were calculated from the assumption of 100 % native soluble proteins in powders at the beginning of storage (*i.e.* time 0 days). Generally speaking, all powders show a similar evolution with comparable percentage of soluble proteins at the end of storage ( $\sim$  85 - 89 %). Also, the impact of oscillation amplitude is negligible with similar profiles for both conditions. Non-native proteins are represented by lactosylated and/or denatured and/or aggregated proteins. Protein lactosylation was also followed as a function of powder storage conditions in Figure 4. For WPC powders, it can first be observed that the lactosylation was slightly more pronounced after large than small oscillations. Examination of mass spectroscopy data revealed that after 16 days and until the end of storage, powders from set 1 were lactosylated to a greater extent than those from set 2. Regarding the  $\beta$ -LG powder, the initial lactosylation rate (*i.e.* lactosylated proteins in the fresh powder) was around 4 % confirming that the successive processes applied to obtain the concentrate and the spray-drying step lead to protein lactosylation. In this case, even if no residual lactose can be detected in the powder, the lactosylated proteins can continue their chemical evolution through the Maillard reaction when stored, explaining the slight evolution of BI observed in 3.1.2 and the frequency of lactose per proteins decrease observed in Figure 4. Norwood et al., (2016) demonstrated for

they powders that the level of lactosylated proteins increased during the first months of storage reaching a maximum, then decreased with storage time. The decrease in protein lactosylation was only observed for  $\beta$ -LG powder and concomitant with the slight increase in BI. It is hypothesised that  $\beta$ -LG proteins were first modified by lactosylation before storage and then degraded in advanced MR products contributing to the powder browning. As no lactose is present in this powder, the extent of lactosylation during storage could not increase as observed for WPC A and B.

### 3.2. Impact of storage on rehydration properties

There is a general consensus that the rehydration process consists of four main steps: wetting, sinking/swelling, dispersion and solubilization (Forny et al., 2011; Gaiani et al., 2009; Mitchell et al., 2015).

Powder wetting is the first step and is determined by the replacement of the gaseous phase by water at the powder surface. In the present study, it was experimentally measured for all powders storage. All powders were found to be non-wettable (time > 1800 s). This result (*i.e.* non wettable) is already well known in the literature for powders of similar composition. In general terms, whey protein powders show poor wetting behaviour with powder material floating on the surface of the solution, which is considered to be the rate-limiting factor particularly for whey proteins (Gaiani et al., 2009). Powders with high protein contents comprise a hydrophobic surface, leading to poor wettability (Nijdam and Langrish, 2006; Wu et al., 2020). Also wetting is found to be more efficient for large particles (at least over 90  $\mu\text{m}$ ) or agglomerated powders (Fournaise et al., 2021; Freudig et al., 1999). Increased particle size results in lower particle-solvent contact angle, thus facilitating wetting. In this work, the median particle size is around 70.53 (+/- 1.61)  $\mu\text{m}$  which is significantly smaller than 90  $\mu\text{m}$  (data not shown).

Dispersibility is defined as the ability of a powder to disperse into water (including breaking of lumps and agglomerates, along with fragmentation of individual particles). Powder dispersion consists of disintegration of lumps and agglomerates into individual particles (deagglomeration) and release of particle fragments (attrition) (Fang et al., 2011; Forny et al., 2011; Mimouni et al., 2010). These two mechanisms lead to size reduction and increase in specific surface area, further facilitating interactions of the solid matrix with water. The results for powder dispersibility are presented in Figure 5-A. The dispersibility was different



for WPC and  $\beta$ -LG powders. Dispersibility of WPC (mean of WPC A and B) was found between 27 and 38 % whereas it was lower for  $\beta$ -LG powders (around 8 - 10 %). The impact of the storage amplitude (large or small oscillations) was not observed for these powders with no significant differences. Generally speaking, the dispersibility was low for all powders. Particle dispersion occurs when the cohesion between particle components is overwhelmed by shear forces exerted by the liquid. As all powders rich in proteins, WPC powders are known to be cohesive due to the hydrophobicity of the compounds (Cuq et al., 2011; Vos et al., 2016). Therefore, these experimental results were expected. Surprisingly, all dispersibility values are slightly improved for powders at the middle of the storage duration. Even if these results were significant, they are hardly explainable.

Solubilization is the final critical step in the rehydration process considered as determinant (Vos et al., 2016). The results of powder solubility are presented in **Figure 5-B**. This final step led to the complete loss of particle structure and the final rehydrated product consists in a suspension of insoluble components (Gaiani et al., 2009; Vos et al., 2016). Here, the solubility of all powders was found close to 100 % (ranging from 98.4 to 99.8 %) with no significant differences regardless of the chemical composition, the oscillations amplitude or the storage duration. Usually, the presence of proteins is known to decrease the solubilization rate. It has been observed particularly for caseins (Fang et al., 2011) but not for whey proteins even if lactosylated and/or aggregated (Paul et al., 2022).

It can be concluded, that the powder rehydration (wettability, solubility and dispersibility) was not strongly affected by both storage duration and oscillations amplitude. In other words, either protein modifications do not impact powder rehydration at the macroscale or the proteins were not modified enough to impact the macroscopic behaviour.

### 3.3. Impact of storage on surface properties

To determine the evolution of surface properties during storage, AFM-based nanoindentation and CFM are relevant and sensitive techniques to give accurate and quantitative data on the different samples at the local scale of few  $\mu\text{m}$  surface areas (**Figure 6**).

The impact of storage duration and oscillations amplitude was evaluated on nanomechanical properties of WPC and  $\beta$ -LG particles (**Figure 6A1 and 6A2**). Example of maps showing the surface stiffness evolution and representative of the results are presented **Figure 7**. Mechanical properties of particles were investigated in order to evidence a possible link with

storage duration and also temperature/RH oscillations. Indeed, such modifications could result in whey proteins shell formation as previously evidenced in the case of casein powders (Mimouni et al., 2010, Burgain et al., 2016b) but has never been demonstrated for whey-based powders. Here, it seems that the evolution of the elasticity features was slightly different for the two different powders with a slight increase during storage only for WPC powder, meaning that soft regions are becoming stiffer. At the end of storage, WPC powders appeared slightly stiffer with an elastic modulus increasing from 1 up to of 2-3 GPa whereas no significant trend was observed for  $\beta$ -LG where an elastic modulus within the range of 2-2.5 GPa was measured all along the storage. As **Figure 7** illustrates, strong heterogeneities of stiffness appearing during storage which can be associated with the formation of stiff patches or domains within a softer surrounding matrix. These stiff patches seem to be randomly distributed over a surrounding matrix of about 0.5 up to 1.0 GPa resulting in a broader elasticity distribution. The mechanical changes observed in WPC and  $\beta$ -LG particles might be related to the fact that the storage, even at 25 °C, stimulates the formation of aggregates leading to heterogeneity in particles stiffness (Anema et al., 2006; Burgain et al., 2017). In particular, the elastic modulus describes the internal organization of various components forming the material. Thus, the protein aggregation is a result of non-covalent interactions (hydrophobic) between these components that harden the surface while the drying process results in changes upon moisture removal (Burgain et al., 2016b). The impact of oscillation is negligible as no differences were observed between large and small oscillations for the same chemical composition.

The evolution of surface hydrophobicity of WPC and  $\beta$ -LG powder particles during storage and under two oscillations amplitudes was measured by CFM (**Figure 6B**). Example of maps showing the surface adhesion evolution and representative of the results are presented in **Figure 8**. First, it appears again that the oscillations amplitude had no impact on either WPC or  $\beta$ -LG particles during the whole storage. As seen in **Figure 6B**, results for large and small oscillations were similar. However, it seems that the evolution of the hydrophobic features during storage was different for these two powders. The surface hydrophobicity was quantified at the nanoscale by mean of CFM with CH<sub>3</sub> terminated AFM tips. Such hydrophobic tips interact with hydrophobic surface which for WPC lead to adhesion peaks on recorded force-distance curves starting from 0.2 nN and reaching values around 0.6 nN at the end of storage. The latter value is close to values obtained from calibration measurements

performed in the same conditions onto hydrophobic alkanethiols substrate (data not shown). Indeed, about 1 nN and 10 nN were respectively measured in ethanol and in water onto this substrate exhibiting contact angle of about 110° as reported in **Alsteens et al. (2007)**. On the contrary, for  $\beta$ -LG particles, the surface hydrophobicity appeared unchanged (hydrophobic forces of about 0.40 nN). The formation of such hydrophobic domains or patches observed for WPC can be linked to the modification of the surface structure that may imply a chemical alteration. Therefore, these results suggest that particle surface property modifications may be related to molecular organization/migration and chemical reactions occurring at the surface of WPC powders only. It can be hypothesised that increase in surface hydrophobicity arise from lipid migration to surface (1), protein unfolding following lactosylation (2) leading to exposure of hydrophobic amino acid residues at particle surface.

To sum-up, the oscillation amplitude during storage had no impact on the surface properties of particles (WPC and  $\beta$ -LG) under the conditions tested. But for WPC powders, storage duration induces heterogeneities at the particle surface for both the surface stiffness and the surface hydrophobicity. Such observation has been already reported by Fyfe and coworkers. They evidenced a strong correlation between the surface hydrophobicity and the chemical composition at the particle surface (**Fyfe et al., 2011**).

## 5. Conclusion

In this paper, powders were monitored under storage conditions mimicking authentic storage whereas most studies are usually performed at constant storage conditions. The objective was to gain an understanding of the impact of the RH and T°C oscillations on their rehydration and physicochemical properties.

Both WPC powders samples tested in this work appear very similar in terms of color evolution (the values are superimposed). The behaviour of these compositionally comparable powders, industrially produced in independent batches, means that the ageing is reproducible between productions. This is particularly important for whey ingredient producers as when predicting the powder shelf life, the proposed model must reasonably fit the behaviour of all of their products.

Under the conditions tested, the oscillation amplitude in RH and temperature during storage had no impact on the measured properties (*i.e.* surface local properties, rehydration ability, protein denaturation, color). The only difference observed is the quantity of lactosylated

proteins slightly higher for large oscillation. On the contrary, storage duration even under low oscillations (mean temperature 25°C) had an impact on lactosylation and Maillard products. It can also be concluded that the rate of lactosylated proteins in the fresh product should be carefully monitored as it will be able to evolved into Maillard products later during product storage, even for powders depleted in lactose such as  $\beta$ -LG powders.

## 6. Acknowledgements

The authors acknowledge support of the LIBio project of the "Lorraine Université d'Excellence" (Investissements d'avenir – ANR 15-004). We would like to thank Lucas Charois and Alexandre Olry, members of the Experimental phytotronic platform of Lorraine PEPLor, Université de Lorraine, France for their technical assistance. We also thank the Spectroscopy and Microscopy Service Facility (SMI) of LCPME (Université de Lorraine-CNRS – <http://www.lcpme.cnrs-nancy.fr>) for technical support in AFM and XPS.

## 7. Conflict of interest

The authors declare that there is no conflict of interest. C. Ray and M. Alexander are employees of Arla Foods Ingredients Group P/S.

## 8. References

AFNOR (2004). Microbiology of food and animal feeding stuffs - Determination of water activity, ISO 21807:2004.

Alsteens, D., Dague, E., Rouxhet, P.G., Baulard, A.R., & Dufrene, Y.F. (2007). Direct measurement of hydrophobic forces on cell surfaces using AFM, *Langmuir*, 23(24), 11977-9.

Anema, S.G., Pinder, D.N., Hunter, R.J., & Hemar, Y. (2006). Effects of storage temperature on the solubility of milk protein concentrate (MPC85), *Food Hydrocolloids*, 20(2), 386–393.

Baisier, W.M., & Labuza, T.P. (1992). Maillard browning kinetics in a liquid model system, *Journal of Agricultural and Food Chemistry*, 40(5), 707-713.

Baldwin, A., Higgs, K., Boland, M., & Schuck, P. (2020). Effects of drying and storage on milk proteins, in *Milk proteins: from expression to food*, Edited by Boland, M., & Singh, H., Elsevier, Pages 423-466.

Borocz, P., Singh, P., & Singh, J. (2015). Evaluation of Distribution Environment in LTL Shipment Between Central Europe and South Africa, *Journal of Applied Packaging Research*, 7(2), 45-60.

Burgain, J., El Zein, R., Scher, J., Petit, J., Norwood, E.A., Francius, G. & Gaiani, C. (2016a). Local modifications of whey protein isolate powder surface during high temperature storage, *Journal of Food Engineering*, 178, 39-46.

Burgain, J., Scher, J., Petit, J., Francius, G., & Gaiani, C. (2016b). Links between particle surface hardening and rehydration impairment during micellar casein powder storage, *Food Hydrocolloids*, 61, 277-285.

Burgain, J., Petit, J., Scher, J., Rasch, R., Bhandari, B., & Gaiani, C. (2017). Surface chemistry and microscopy of food powders, *Progress in surface science*, 92(4), 409-429.

Csavajda, P. & Böröcz, P. (2019). Climate Conditions in ISO Container Shipments from Hungary to South Africa and Asia, *Periodica Polytechnica Transportation Engineering*, 47(3), 233–241.

Cuq, B., Rondet, E. & Abecassis, J. (2011). Food powders engineering, between knowhow and science: Constraints, stakes and opportunities, *Powder Technology*, 208(2), 244-251.

O'Donoghue, L.T., Haque, M.K., Hogan, S.A., Laffir, F.R., O'Mahony, J.A., Murphy, E.G. (2020). Dynamic Mechanical Analysis as a Complementary Technique for Stickiness Determination in Model Whey Protein Powders, *Foods*, (9), 1295.

Fang, Z. & Bhandari, B. (2012). 4 - Spray drying, freeze drying and related processes for food ingredient and nutraceutical encapsulation, in *Encapsulation Technologies and Delivery Systems for Food Ingredients and Nutraceuticals*, Edited by Garti, N., & McClements, D.J., Woodhead Publishing, Pages 73-109.

Fang, Y., Selomulya, C., Ainsworth, S., Palmer, M. & Chen, X.D. (2011). On quantifying the dissolution behaviour of milk protein concentrate, *Food Hydrocolloids*, 25(3), 503-510.

Folch, J., Lees, M. & Stanley, G.H.S. (1957). A simple method for the isolation and purification of total lipids from animal tissues, *Journal of Biological Chemistry*, 226(1), 497-509.

Forny, L., Marabi, A. & Palzer, S. (2011). Wetting, disintegration and dissolution of agglomerated water-soluble powders, *Powder Technology*, 206(1), 72–78.

Fournaise, T., Petit, J. & Gaiani, C. (2021). Main powder physicochemical characteristics influencing their reconstitution behaviour, *Powder Technology*, 383, 65-73.

Freudig, B., Hogekamp, S. & Schubert, H. (1999). Dispersion of powders in liquids in a stirred vessel, *Chemical Engineering and Processing – Process Intensification*, 38(4-6), 525-532.

Fyfe, K.N., Kravchuk, O., Le, T., Deeth, H.C., Nguyen, A.V. & Bhandari, B. (2011). Storage induced changes to high protein powders: influence on surface properties and solubility, *Journal of the Science of Food and Agriculture*, 91(14), 2566-2575.

Gaiani, C., Scher, J., Schuck, P., Desobry, S. & Banon, S. (2009). Use of a turbidity sensor to determine dairy powder rehydration properties, *Powder Technology*, 190(1-2), 2-5.

Gaiani, C., Omar, R., El-Kirat-Chatel, S., Cvetkovska, L., Alexander, M., Ray, C., Burgain, J. & Francius, G. (2021). Atomic force microscopy nanoscale analysis: Impact of storage conditions on surface properties of whey protein powders, *Food Hydrocolloids*, 118, 106801.

Gazi, I. & Huppertz, T. (2015). Influence of protein content and storage conditions on the solubility of caseins and whey proteins in milk protein concentrates, *International Dairy Journal*, 46, 22–30.

Guyomarc'h, F., Warin, F., Donald Muir, D. & Leaver, J. (2000). Lactosylation of milk proteins during the manufacture and storage of skim milk powders, *International Dairy Journal*, 10(12), 863–872.

IDF (1979). Determination of the dispersibility and wettability of instant dried milk, *International Dairy Federation*, Brussels, Belgium.

IDF (2005). Dried milk and dried milk products—Determination of insolubility index, *International Dairy Federation*, Brussels, Belgium.

Mimouni, A., Deeth, H.C., Whittaker, A.K., Gidley, M.J. & Bhandari, B.R. (2010). Investigation of the microstructure of milk protein concentrate powders during rehydration: Alterations during storage, *Journal of Dairy Science*, 93(2), 463-472.

Mitchell, W.R., Forny, L., Althaus, T.O., Niederreiter, G., Palzer, S., Hounslow, M.J. & Salman, A.D. (2015). Mapping the rate-limiting regimes of food powder reconstitution in a standard mixing vessel, *Powder Technology*, 270, 520-527.

Mortensen, A.B. & Wallin, H. (1898). Gravimetric determination of ash in food, *Journal of the Association of Official Analytical Chemists*, 72(3), 481-483.

Nijdam, J.J. & Langrish, T.A.G. (2006). The effect of surface composition on the functional properties of milk powders, *Journal of Food Engineering*, 77(4), 919-925.

Nikolova, Y., Petit, J., Sanders, C., Gianfrancesco, A., Scher, J. & Gaiani, C. (2015). Toward a better determination of dairy powders surface composition through XPS matrices development, *Colloids and Surfaces – B : Biointerfaces*, 125, 12-20.

Nishanthi, M., Chandrapala, J. & Vasiljevic, T. (2018). Physical properties of selected spray dried whey protein concentrate powders during storage, *Journal of Food Engineering*, 219, 111-120.

Norwood, E.-A., Chevallier, M., Le Floch-Fouéré, C., Schuck, P., Jeantet, R. & Croguennec, T. (2016). Heat-induced aggregation properties of whey proteins as affected by storage conditions of whey protein isolate powders, *Food and Bioprocess Technology*, 9(6), 993–1001.

Norwood, E.-A., Pezennec, S., Burgain, J., Briard-Bion, V., Schuck, P., Croguennec, T., Jeantet, R. & Le Floch-Fouéré, C. (2017). Crucial role of remaining lactose in whey protein isolate powders during storage, *Journal of Food Engineering*, 195, 206–216.

Paul, A., Gaiani, C., Cvetkovska, L., Paris, C., Alexander, M., Ray, C., Francius, G., EL-Kirat-Chatel, S. & Burgain, J. (2022). Deciphering the impact of whey protein powder storage on protein state and powder stability, *Journal of Food Engineering*, in press.

Polyakov, P., Soussen, C., Duan, J., Duval, J.F.L., Brie, D. & Francius, G. (2011). Automated force volume image processing for biological samples, *PLoS One*, 6(4), e18887.

Schuck, P., Dolivet, A. & Jeantet, R. (2012). Analytical methods for food and dairy powders, *John Wiley and Sons*, pp 228.

Schuck, P., Jeantet, R., & Kelly, P. (2016). Recent advances in spray drying relevant to the dairy industry: A comprehensive critical review, *Drying Technology*, 34(15), 1773-1790.

Sharma, A., Jana, A.H. & Chavan, R.S. (2012). Functionality of Milk Powders and Milk-Based Powders for End Use Applications-A Review, 11(5), 518-528.

O'Sullivan, J.J., Norwood, E.A., O'Mahony, J.A. & Kelly, A.L. (2019). Atomisation technologies used in spray drying in the dairy industry: A review, *Journal of Food Engineering*, 243, 57-69.



Tunick, M.H., Thomas-Gahring, A., Van Hekken, D.L., Landola, S.K., Singh, M., Qi, P.X., Ukuku, D.O., Mukhopadhyay, S., Onwulata, C.I. & Tomasula, P.M. (2016). Physical and chemical changes in whey protein concentrate stored at elevated temperature and humidity, *Journal of Dairy Science*, 99(3), 2372-2383.

Vos, B., Crowley, S.V., O'Sullivan, J., Evans-Hurson, R., McSweeney, S., Kruse, J., Ahmed, M.R., Fitzpatrick, D. & O'Mahony, J.A. (2016). New insights into the mechanism of rehydration of milk protein concentrate powders determined by Broadband Acoustic Resonance Dissolution Spectroscopy (BARDS), *Food Hydrocolloids*, 61, 933-945.

Wu, S., Fitzpatrick, J., Cronin, K., Maidannyk, V. & Miao, S. (2020). Effects of spraying surfactants in a fluidised bed on the rehydration behaviour of milk protein isolate powder, *Journal of Food Engineering*, 266, 109694.

## Figures Caption

**Figure 1.** Experimental conditions programmed to fit large oscillations (ranges T: 20-30°C; RH: 65-75) and small oscillations (ranges T: 22.5-27.5°C; RH: 67.5-72.5).

**Figure 2.** Browning index and photo of petri dishes during storage of WPC (A), WPC (B) and  $\beta$ -LG powders (large oscillations ranges T: 20-30°C; RH: 65-75 and small oscillations ranges T: 22.5-27.5°C; RH: 67.5-72.5).

**Figure 3.** Solubles proteins (%) evolution for WPC and  $\beta$ -LG powders during storage (Large oscillations ranges T: 20-30°C; RH: 65-75 and Small oscillations ranges T: 22.5-27.5°C; RH: 67.5-72.5).

**Figure 4.** Frequency (%) of lactosylated proteins (1, 2, 3 and 4 lactoses) for WPC and  $\beta$ -LG powders during storage (Large oscillations ranges T: 20-30°C; RH: 65-75 and Small oscillations ranges T: 22.5-27.5°C; RH: 67.5-72.5).

**Figure 5.** Powder dispersibility (A) and solubility (B) for WPC (1) and  $\beta$ -LG (2) powders during storage under the two oscillations (Large oscillations ranges T: 20-30°C; RH: 65-75 and Small oscillations ranges T: 22.5-27.5°C; RH: 67.5-72.5).

**Figure 6.** Surface characterization by AFM (A: Elasticity, B: Hydrophobicity) for WPC (1) and  $\beta$ -LG (2) powders (Large oscillations ranges T: 20-30°C; RH: 65-75 and Small oscillations ranges T: 22.5-27.5°C; RH: 67.5-72.5).

**Figure 7.** Example of representative maps showing the surface stiffness evolution during storage for WPC and  $\beta$ -LG powders.

**Figure 8.** Example of representative maps showing surface adhesion evolution during storage for WPC and  $\beta$ -LG powders.

## Table caption

**Table 1.** Chemical composition<sup>1</sup> for WPC (A), WPC (B) and  $\beta$ -LG powders.

<sup>1</sup> n=3 for all experiments except for detailed proteins (n=2)

<sup>2</sup> Data coming from industrial partner

### SUPPLEMENTARY MATERIAL

**Supplementary Material 1.** Powder shipping real data recorded during transport from Amsterdam to India (personnal data from AFI, Videbæk, Denmark).

**Supplementary Material 2.** Raw data recorded during powder storage into the phytotrons and corresponding to large (T: 20-30°C; RH: 65-75) and small oscillations (T: 22.5-27.5°C; RH: 67.5-72.5).

FIGURE 1

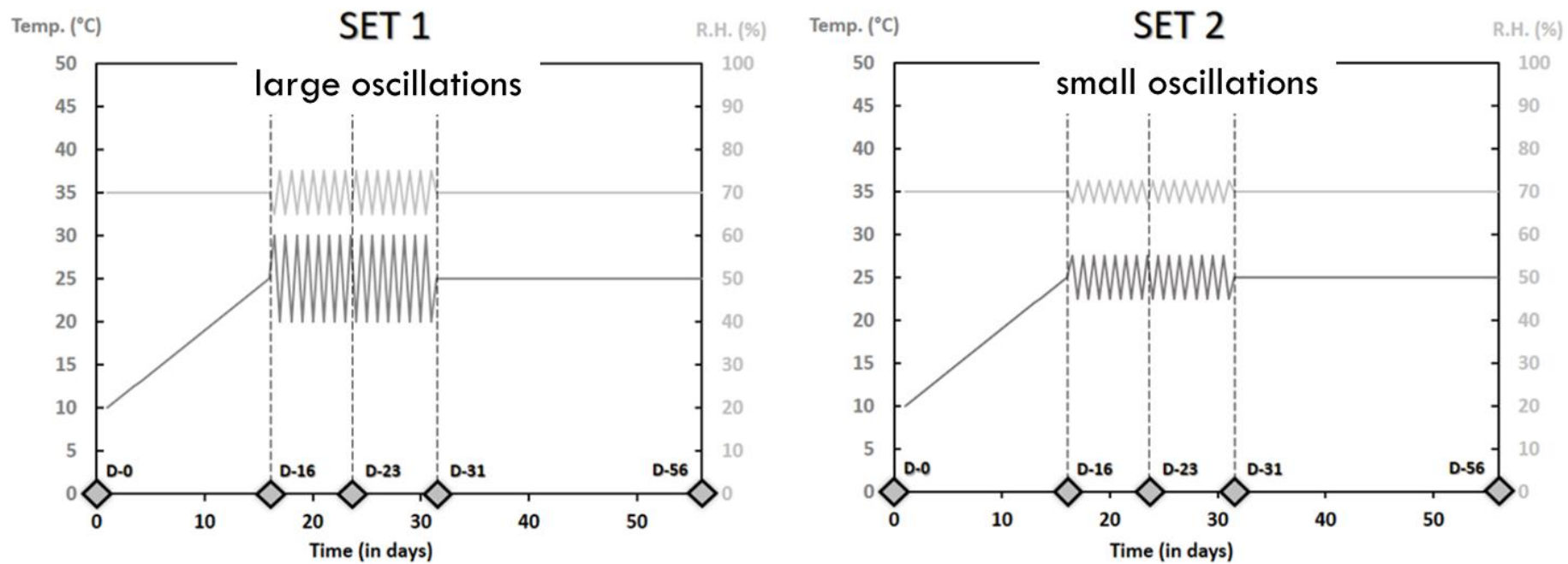


FIGURE 2

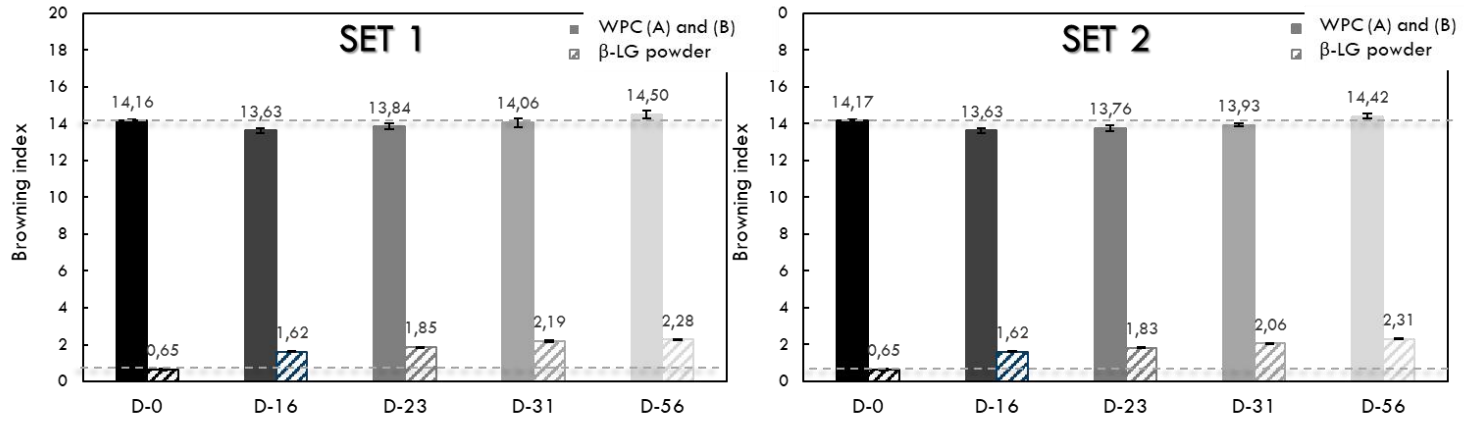
**A****B**

FIGURE 3

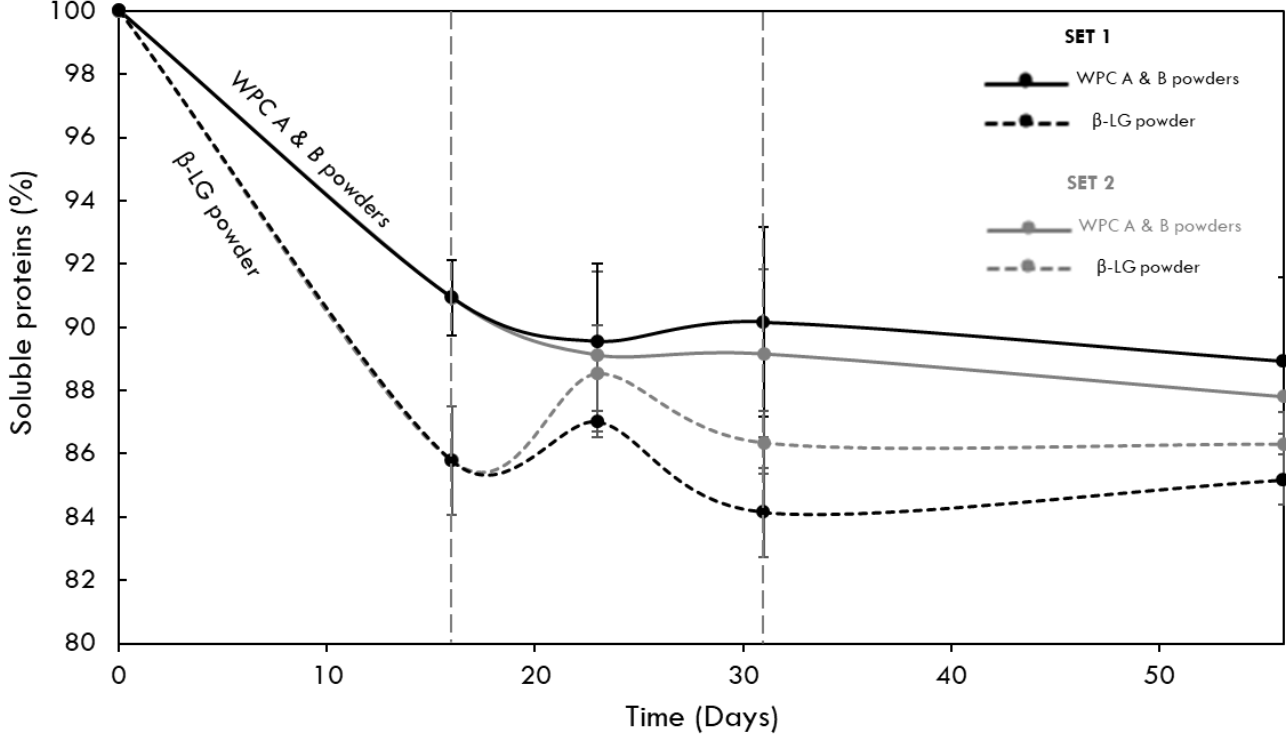
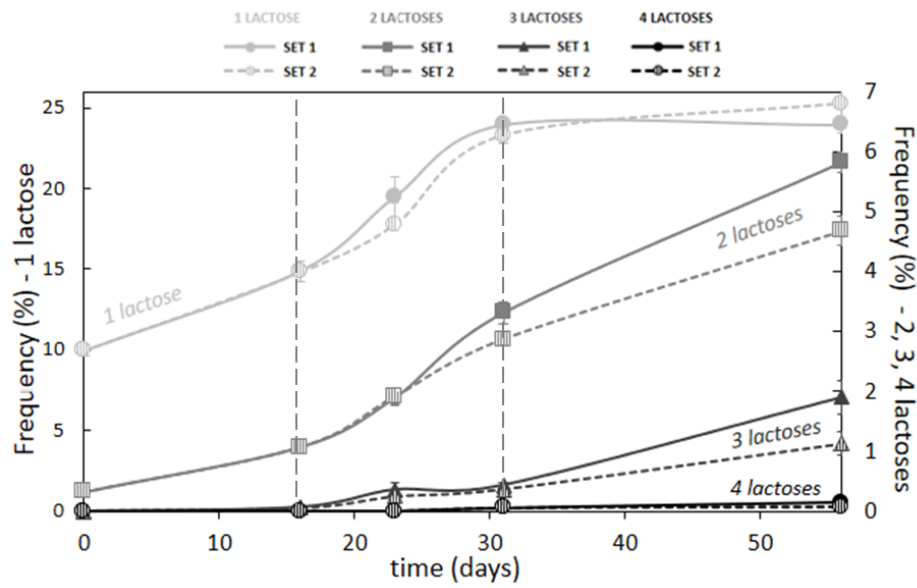


FIGURE 4

WPC (A) and (B) powders



$\beta$ -LG powder

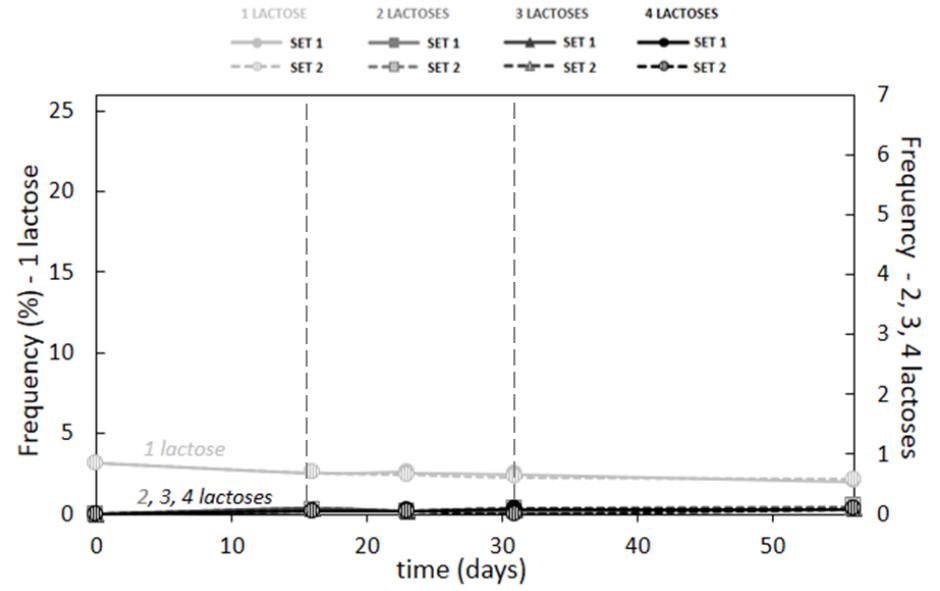


FIGURE 5

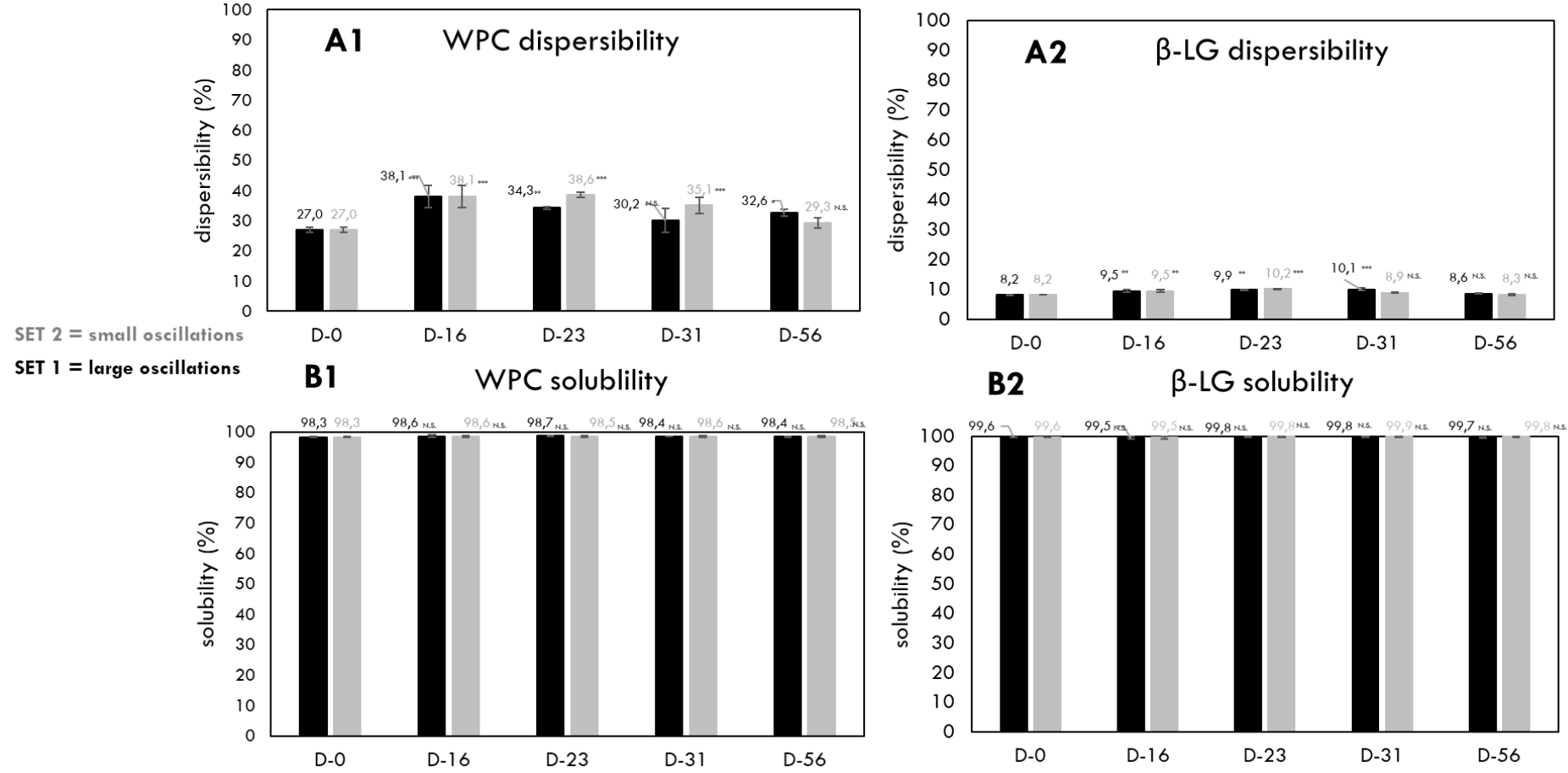


FIGURE 6



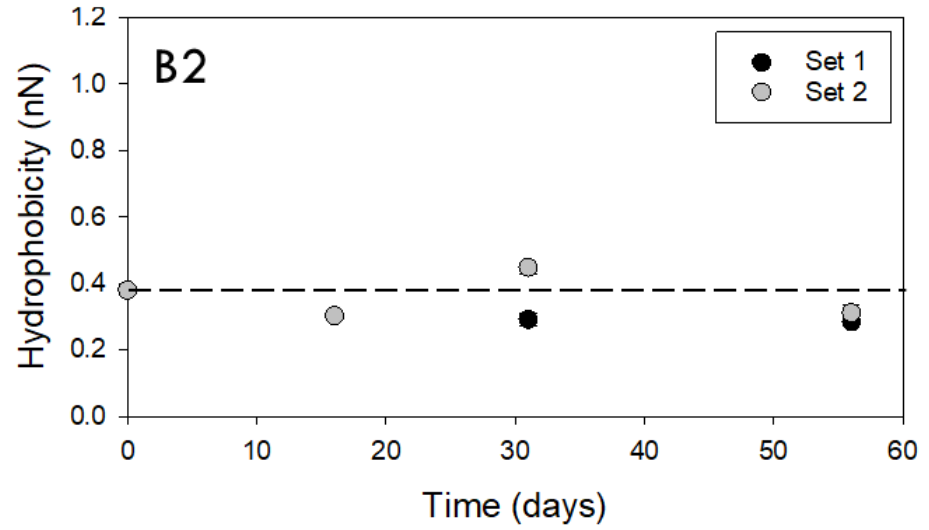
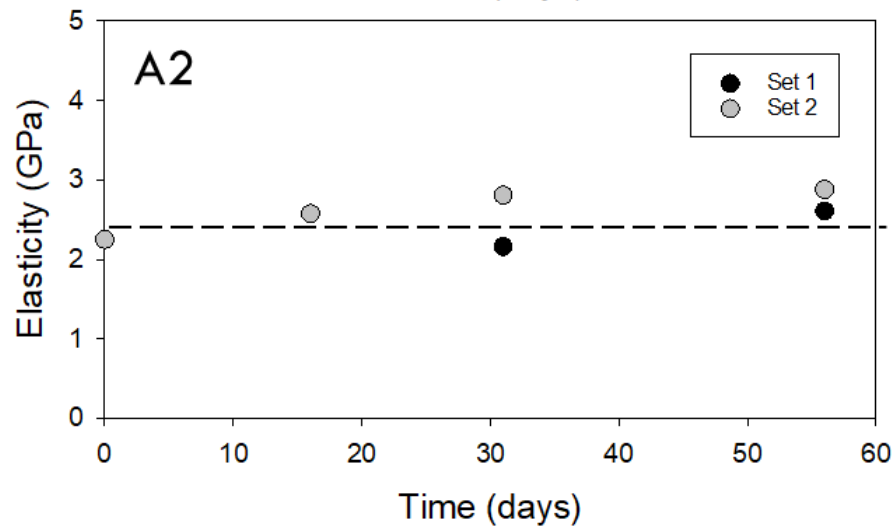
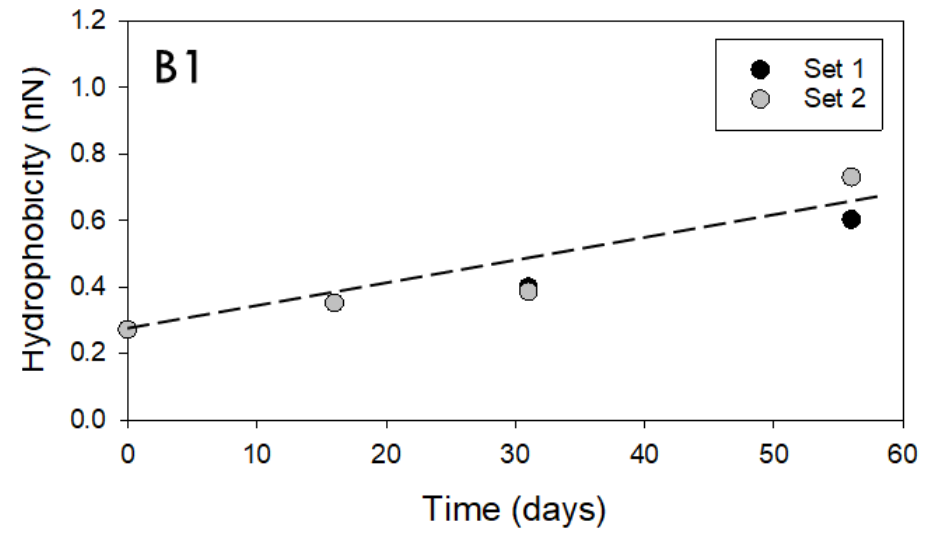
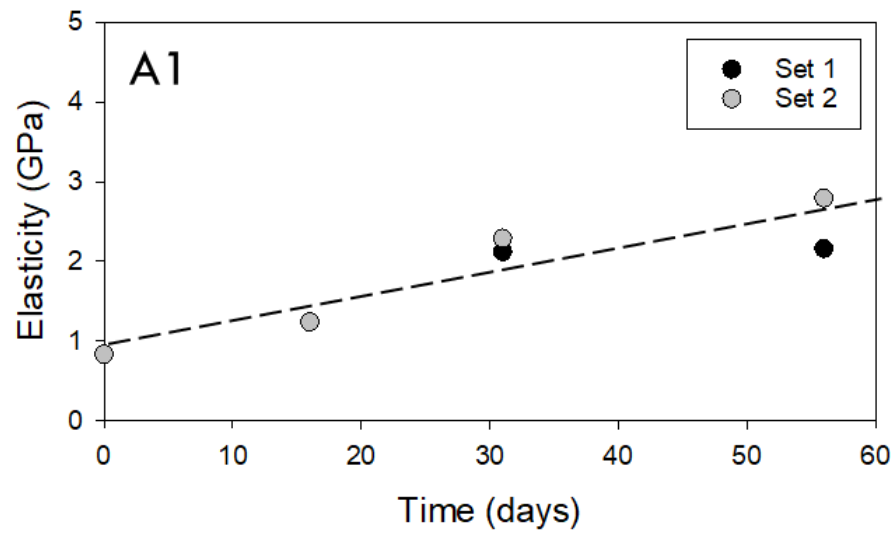


FIGURE 7

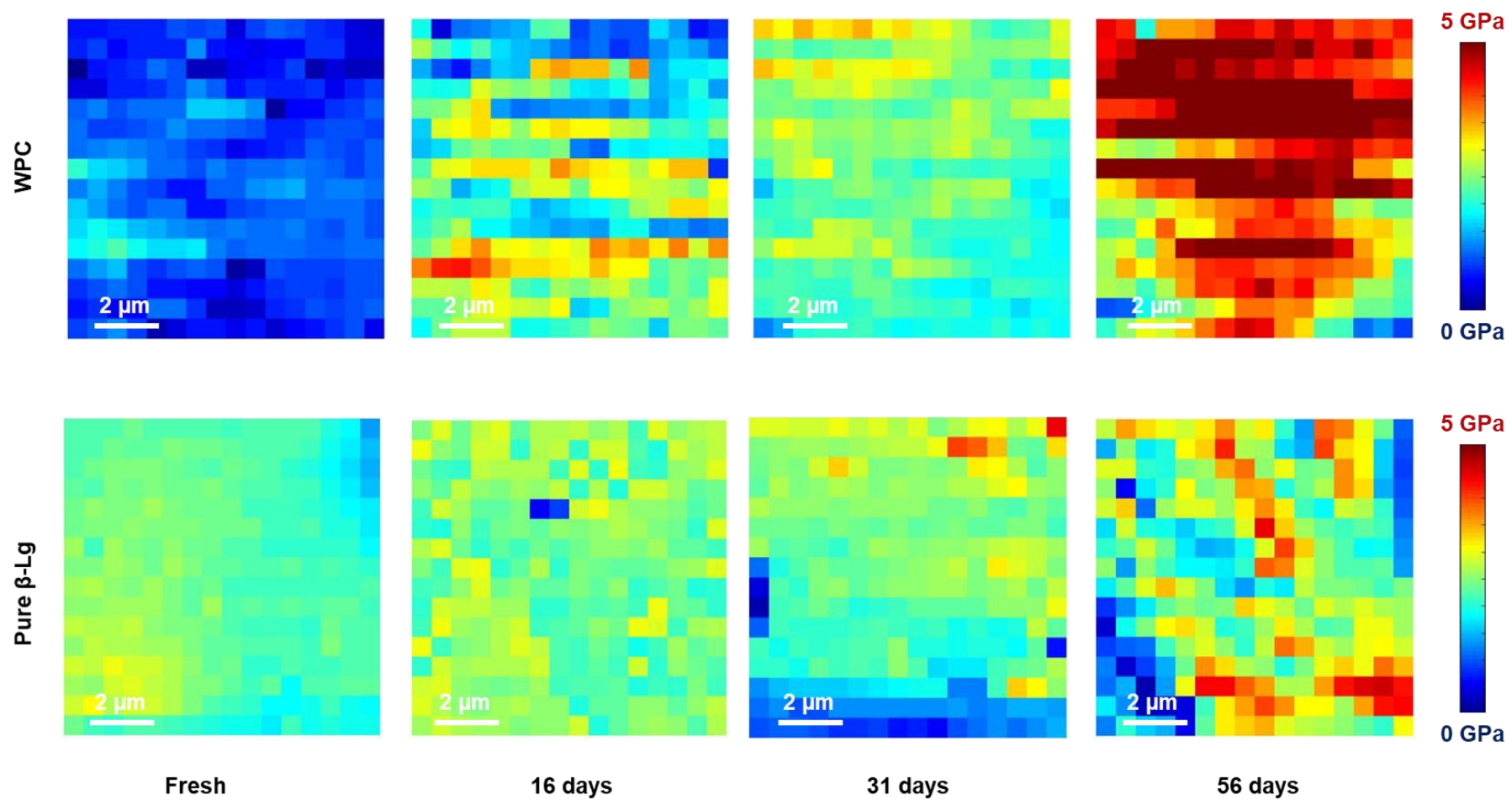
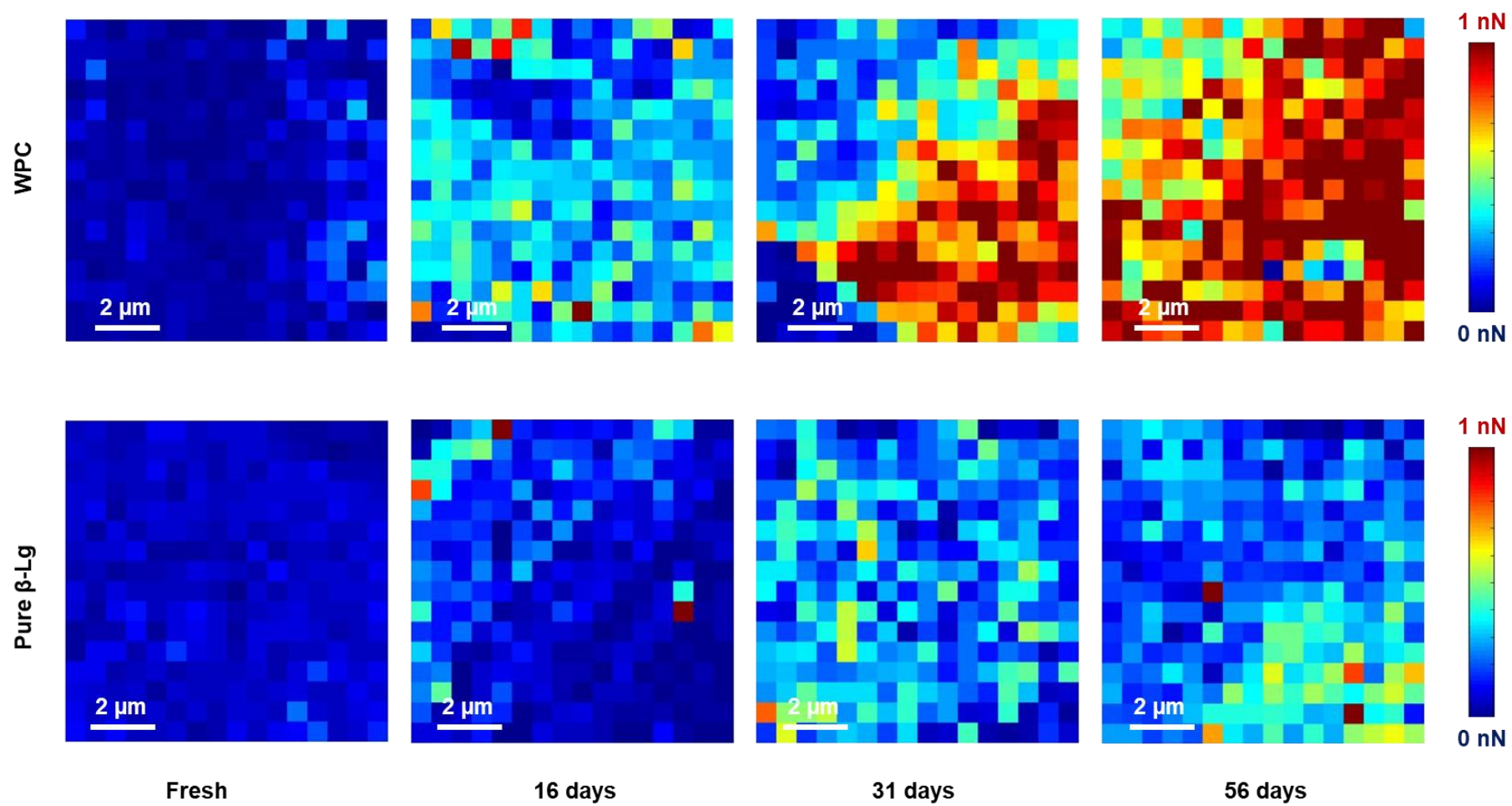
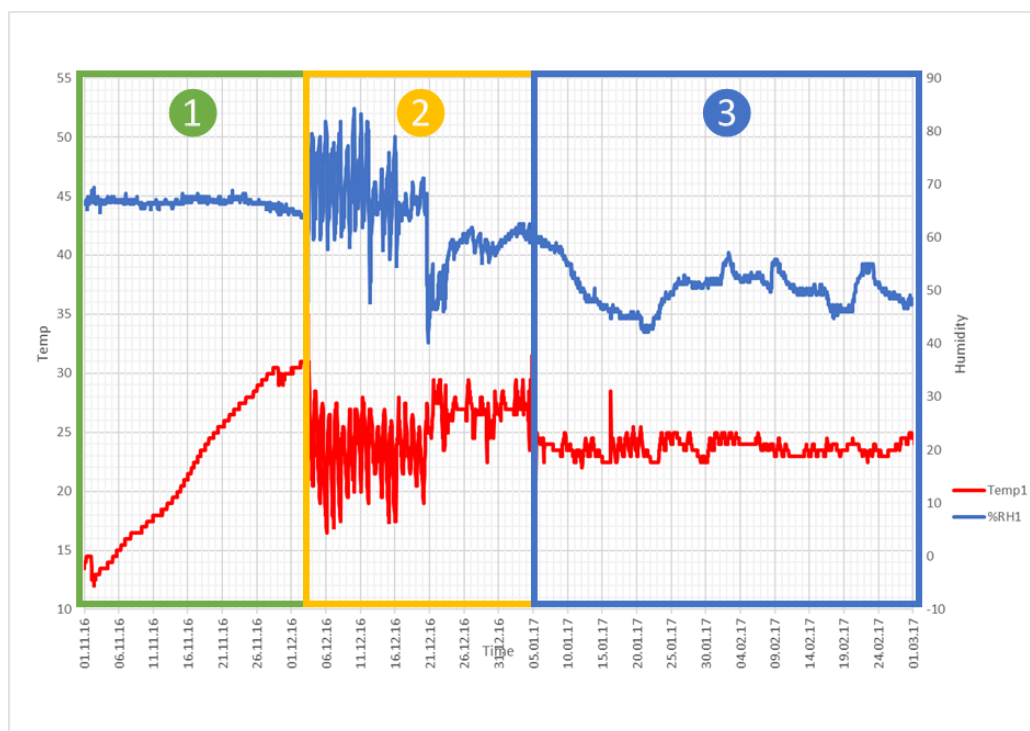


FIGURE 8



## SUPPLEMENTARY MATERIAL 1

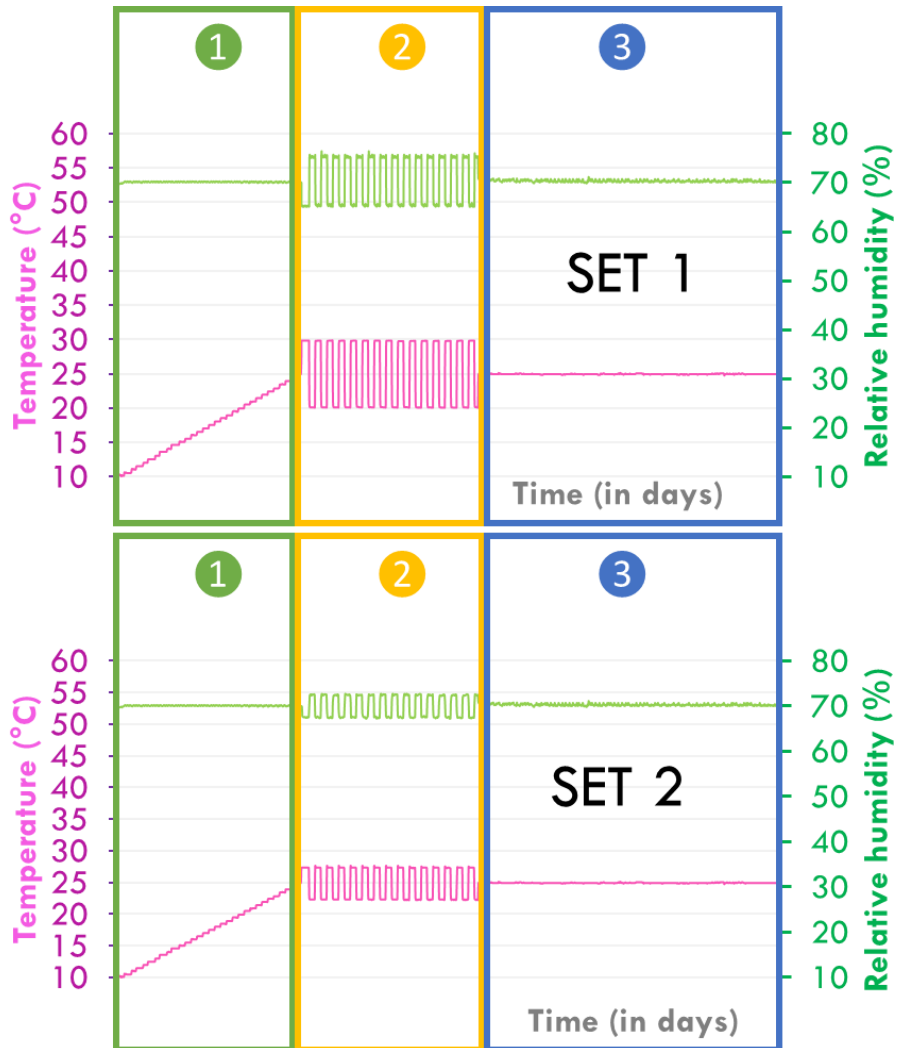


1  
Temperature ramp  
Constant relative humidity

2  
Temperature oscillation  
Relative humidity oscillation

3  
Constant temperature  
Constant relative humidity

## SUPPLEMENTARY MATERIAL 2



1  
 Temperature ramp  
 Constant relative humidity

2  
 Temperature oscillation  
 Relative humidity oscillation

3  
 Constant temperature  
 Constant relative humidity

TABLE 1

Composition in (g.100g-1)	WPC (A)	WPC (B)	$\beta$ -LG
<b>Lipids</b>	3.9 $\pm$ 0.3	4.7 $\pm$ 0.1	-
<b>Lactose</b> <sup>2</sup>	1.5	1.5	-
<b>Ashes</b>	2.4 $\pm$ 0.0	2.6 $\pm$ 0.3	2.3 $\pm$ 0.1
<b>Water</b>	5.5 $\pm$ 0.0	5.5 $\pm$ 0.1	4.6 $\pm$ 0.1
<b>Total proteins</b>	74.8 $\pm$ 0.8	76.8 $\pm$ 0.9	83.9 $\pm$ 3.9
Caseins (% of total proteins)	-	-	-
$\beta$ -LG (A) (% of total proteins)	25.1 $\pm$ 0.4	24.9 $\pm$ 0.4	31.6 $\pm$ 0.1
$\beta$ -LG (B) (% of total proteins)	46.9 $\pm$ 0.3	46.7 $\pm$ 0.4	68.4 $\pm$ 0.4
$\alpha$ -LA (% of total proteins)	28.0 $\pm$ 0.3	28.3 $\pm$ 0.2	-

<sup>1</sup> n=3 for all experiments except for detailed proteins (n=2)

<sup>2</sup> Data coming from industrial partner